Dynamical critical phenomena in ND_4Br †

Y. Yamada* and Y. Noda
College of General Education, Osaka University, Toyonaka, Osaka, Japan

J. D. Axe and G. Shirane
Brookhaven National Laboratory,‡ Upton, New York 11973

(Received 30 October 1973)

The dynamical critical phenomena associated with the structural phase transition of ND_4Br (T_c = 215 °K) have been studied by neutron-scattering techniques. The measurements of the low-energy part of neutron spectra of ND_4Br single crystals have been carried out along the principal symmetry directions of cubic reciprocal space. The spectra observed along the [110] direction show a "triple-peak" structure. The central (quasielastic) component is clearly due to the coupled relaxational motion of displacement of Br^- ions and the flipping of ND_4^+ ions. The width Γ (full width at half-maximum) of the central component is less than the instrumental resolution ($\Gamma_{cent} \leq 0.28$ meV). In addition to the central component, there exists a well-defined TA_2 phonon mode at the [110] zone boundary whose eigenvector exactly corresponds to the spontaneous displacement of Br^- ions in the low-temperature phase. However, this phonon mode does not show any appreciable softening nor broadening throughout the temperature region of $220 < T < 295$ °K. Rather the intensity of the central component at the M point critically increases. These experimental results are analyzed by looking upon the system as a pseudospin-phonon coupled system. It is shown that the observed neutron spectra $S(\mathbf{K}, \omega)$ are satisfactorily explained with such a formalism by taking the relaxation time of the flipping of an independent ammonium ion longer than 1.3×10^{-12} sec. The distribution of intensity of the central peak shows two maxima in the reciprocal space, one at the Γ point (zone center) and another at the M point ([110] zone boundary). This gives direct evidence for the existence of the two competitive interactions: direct interaction between ammonium ions and indirect interaction via phonon modes. This competition is postulated to explain the two successive phase transitions which occur in ND_4Br.

I. INTRODUCTION

Structural phase transitions are usually classified into two classes. (a) Order-disorder type: The possible positions of atoms are spatially discrete, and the variable which plays the role of the order parameter is described by a pseudospin variable. The phase transition in this case is interpreted in terms of cooperative ordering of the spin system. (b) Displacive type: The displacement of atoms are described by spatially continuous variables. The kinetic energy plays an important part in the total Hamiltonian. In this case, the phase transition is interpreted in terms of instability of a particular phonon mode.

In addition to these, there are other interesting cases when these two types of variables coexist in the crystal, and the condensation of the phonon mode and the long-range ordering of the pseudospin take place at the same time due to strong coupling between them. We may classify this case as (c) a pseudospin-phonon coupled case. The properties of the phase transitions belonging to this class have been investigated mainly in connection with Jahn-Teller phase transitions[1–3] and ferroelectric phase transitions triggered by the ordering of the proton system.[4,5] Another simple example of the coupled system is given by several crystals containing molecular groups. It commonly happens that the orientational order of molecular groups takes place accompanied by the condensation of phonon modes. Ammonium halides, especially NH_4Br, provides a typical example of such a coupled system.

The NH_4Br crystal (CsCl structure) undergoes two successive phase transitions at 235 and 108 °K associated with the orientational ordering of NH_4^+ ionic group. As is usually done, let us attribute a classical Ising variable (pseudospin) to specify the two possible orientations of NH_4^+ ion. Then the structure in the lowest temperature phase (δ phase) is characterized by parallel ordering of pseudospins and that in the intermediate phase (γ phase) is characterized by ($\pi\pi 0$)-type antiparallel arrangement of pseudospins. The highest-temperature phase (β phase) is the disordered phase in which each pseudospin is oriented randomly into "up" or "down" states.[6] Since the pioneering theoretical work by Nagamiya on ammonium halides,[7,8] extensive studies on the phase transitions of this substance have been performed with various experimental techniques. In addition to the above stated crystal-structure analysis, precise measurements of the temperature dependences of the lattice parameters[9] and the long-range-order parameter[10,11] were carried out by x-ray and neutron diffraction. The critical diffuse scattering of neutrons due to spin fluctuations was observed by Seymour.[12] The

properties of the ultrasonic propagation were studied by Garland and Yarnell[13] with specific reference to the critical behavior at the β-γ transition point. NMR measurements[14–16] were also carried out to investigate the dynamical properties of the ammonium ions. Anomalies in Raman spectra around the transition point were also studied by Wang.[17] Most of these investigations were made considering the system as an Ising spin system. It should be noticed, however, that in the γ phase spontaneous displacement of Br^- ions from the high-symmetry site take place along with the antiparallel ordering of the pseudospin.[18] The pattern of the small displacement exactly corresponds to the eigenvector of the TA_2 phonon at the [110] zone boundary; that is, this particular phonon mode can be said to condense in the γ phase. Moreover, the amount of the spontaneous Br^- displacement is proportional to the long-range-order parameter of the pseudospin[11] throughout the γ phase. These facts clearly show that the system should be treated as an pseudospin-phonon coupled system. Recently, Yamada, Mori, and Noda[19] developed a microscopic theory of the successive phase transitions in NH_4Br by taking into account the effect of the spin-phonon coupling explicitly. They have shown that the antiparallel ordering accompanied by the spontaneous displacement of the Br^- ions is stabilized by the spin-phonon coupling energy, whereas the parallel ordering is stabilized by the direct spin-spin coupling.

In the theory developed in Ref. 19, it is assumed that the property of the coupled system is described by a microscopic Hamiltonian

$$H=\frac{1}{2}\sum_{\vec{k},s}(P^2_{\vec{k},s}+\omega_0^2 Q^2_{\vec{k},s})-\frac{1}{2}\sum_{i,j}J_{ij}\sigma_i\sigma_j + \sum_{\vec{k},s}\frac{\omega_0(\vec{k},s)}{\sqrt{N}}g_{\vec{k},s}Q_{\vec{k},s}\sigma_i e^{i\vec{k}\cdot\vec{r}_i}\quad , \tag{1}$$

where $Q_{\vec{k},s}$ is the normal coordinate of the displacement of the ND_4^+ ion as a unit and the Br^- ion, σ_i is the variable to describe the "spin" state at site i, $\omega_0(\vec{k},s)$ is the characteristic frequency of the phonon with wave vector $\vec{k}$ and mode s, J_{ij} is the pair interaction between the ith spin and the jth spin, and $g_{\vec{k},s}$ is the coupling constant between spins and phonons. $P_{\vec{k},s}$ is the canonical conjugate of $Q_{\vec{k},s}$. Starting from the Hamiltonian given in Eq. (1), various aspects of the static properties of the coupled system such as long-range order of the pseudospin $\langle\sigma(k_0)\rangle$, condensed phonon amplitude $\langle Q(\vec{k}_0)\rangle$, and correlation functions of the spin $\langle|\sigma(\vec{k})|^2\rangle$, can be investigated. In the case of ND_4Br, $\langle\sigma(\vec{k}_0)\rangle$, $\langle Q(\vec{k}_0)\rangle$, and $\langle|\sigma(\vec{k})|^2\rangle$ are directly comparable with the experimental results of neutron (elastic) scattering and x-ray scattering. In Ref. 19 the comparison of experimental results and the theoretical values has been performed with considerable success. In this treatment, however, the dynamical aspects of the phase transition of this system have not been investigated.

As for the dynamical critical behavior of the coupled system, several studies have been done with particular reference to the ferroelectric phase transition of potassium dihydrogen phosphate (KDP).[4,20] (Recently, Pytte[21] and Feder and Pytte[22] treated the dynamical behavior of a Jahn-Teller phase transition.) In the case of KDP, the pseudospin is represented by Pauli spin operator, while in Eq. (1) it is given as a classical Ising spin. Recently, Yamada, Takatera, and Huber[23] developed a general treatment of the dynamical critical behavior when the Hamiltonian is given by Eq. (1). It is based on Onsager's theory[24] of irreversible processes. It has been shown that the dynamical critical behavior of the coupled system shows wide variation depending upon the ratio of the phonon frequency ω_0 and the flipping frequency τ_0^{-1} of the spin. For instance, the spectra of phonon-phonon correlations show either three peaks or two phonon-like peaks corresponding to $\tau_0^{-1}\ll\omega_0$ or $\tau_0^{-1}\gg\omega_0$, respectively. In the former case, critical behavior is mainly seen in the central component, while in the latter, critical softening of the phonon-like peaks occurs. These features are depicted in Fig. 1.

On the other hand, no experimental work has been carried out to investigate the dynamical critical behavior of such a coupled system. Thus many interesting points, such as whether or not the condensing phonon mode becomes soft around the crit-

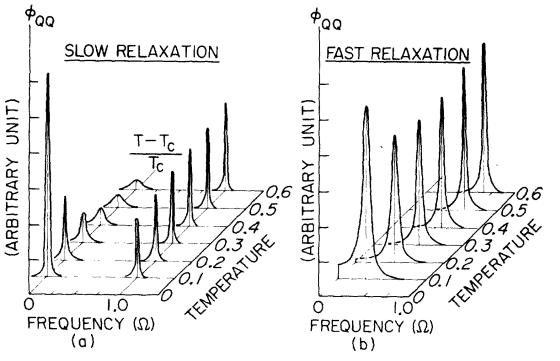

FIG. 1. Phonon-phonon correlation function ϕ_{QQ} plotted against reduced frequency $\Omega\equiv\omega/\omega_0$ and reduced temperature $(T-T_c)/T_c$, where ω_0 and T_c are the characteristic frequency of the phonon and the transition temperature, respectively. Case (a) corresponds to typical patterns when $\tau_0^{-1}\ll\omega_0$, τ_0 being the relaxation time of flipping motion of a independent spin, whereas case (b) corresponds to that when $\tau_0^{-1}\gg\omega_0$. These figures are taken from Ref. 23.

ical temperature in the coupled system, have not been elucidated.

The purpose of the present work is to carry out the measurement of neutron inelastic scattering from a ND_4Br crystal, a typical pseudospin-phonon coupled system, and to investigate the dynamical critical behavior in this substance by analyzing the observed experimental results with the treatment developed in Ref. 23.

II. EXPERIMENTAL

In this experiment the deuterated crystal is necessary for the precise neutron-scattering experiments to eliminate strong incoherent scattering due to the existance of hydrogen atoms. The deuteration process is similar to the method described by Teh and Brockhouse.[26] The aqueous solution was prepared by adding 130 g of NH_4Br to 100 ml of D_2O and then allowed to stay for 24 h at 70 °C to accelerate the deuteration. After the solution was evaporated to obtain a partially deuterated specimen, fresh D_2O was added for further deuteration. This process was repeated seven times. In order to grow the single crystal of ND_4Br from aqueous solution, a habit modifier is necessary to prevent irregular growth. As a habit modifier we used deuterated urea of $\frac{1}{3}$ of ND_4Br in weight. The deuteration of urea was done in the same way as ND_4Br. The mother solution (120 g of ND_4Br, 40 g of ND_2COND_2, and 110 ml of D_2O) was put in a temperature-controlled water bath. The temperature of the water bath was lowered at the rate of 0.1 °C per day. The largest single crystal thus obtained was colorless, having [001] faces and was $7.7\times13.0\times12.2$ mm in size. The degree of deuteration was determined by comparing the proton NMR absorption intensity of the ND_4Br specimen with that of a NH_4Br standard sample. It was shown that more than 95% deuteration was attained in our ND_4Br specimen.

Measurements of inelastic neutron scattering were done on a triple-axis spectrometer at the Brookhaven high-flux-beam reactor. The monochrometer and analyzer were pyrolytic graphite with a 0.4° mosaic spread. The collimation was 20 min on each side of the sample, 40 min between the analyzer and detector, and 40 min before the monochrometer. Most of the measurements were made with constant initial energy of 14.8 meV, and the higher-order contamination was eliminated by the use of pyrolytic graphite filter. The temperature of the sample was kept constant within 0.2 °K.

Although the measurements were carried out in the disordered phase, we could obtain well-defined peaks in neutron spectra corresponding to one-phonon excitations in the low-energy region ($\hbar\omega \lesssim 10$ meV). Several of the observed phonon dispersion curves of low-lying acoustic branches along $[\zeta 00]$, $[0\zeta\zeta]$ and $[\zeta\frac{1}{2}\frac{1}{2}]$ directions are shown in Fig. 2. The branch we are particularly interested in is the lowest-lying TA_2 branch along the $[0\zeta\zeta]$ direction because the zone boundary mode ($\zeta=\frac{1}{2}$) of this branch is the one which "condenses" in the γ phase. In this direction, in addition to peaks corresponding to one-phonon excitations, we observed a quasielastic-scattering cross section centered at $\omega=0$. One of typical neutron spectra obtained at (0, 0.3, 0.3) around the (300) reciprocal-lattice point is shown in Fig. 3. The intensity of the quasielastic component is strongly dependent on the value of ζ. In Fig. 4, the spectra observed at various values of ζ along $[0\zeta\zeta]$ are summarized. These spectra are measured at 295 °K. As $\zeta \to 0.5$ along $[0\zeta\zeta]$ direction, the intensity of the quasielastic component increases markedly. As is shown later, these quasielastic components are directly related to the critical fluctuations of both the ND_4^+ ions and Br^- ions. In order to observe the precise $\vec{k}$ dependence of the intensity of the quasielastic component, we carried out constant-E scanning with $E=0$ along $[\zeta 00]$, $[0\zeta\zeta]$, and $[\zeta\frac{1}{2}\frac{1}{2}]$ directions around the (300) lattice point. The strong Bragg reflection at (300) caused some difficulty in observing the quasielastic component near the Γ point (zone center). Measurements along the $[0\zeta\zeta]$ direction around $\zeta \simeq 0$ suffered particularly from this unfavorable condition, since in our experimental set up ($[0\bar{1}1]$ vertical axis of rotation), the (300) Bragg reflection extended along the $[0\zeta\zeta]$ direction due to mosaic spread of the crystal. This, together with the extended resolution function of neutron probe, gave rise to contamination of Bragg reflection up to

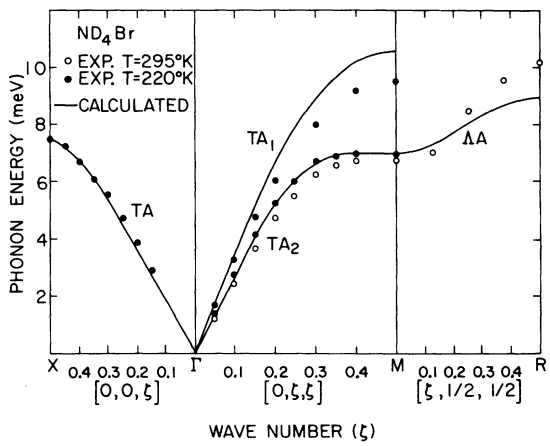

FIG. 2. Low energy phonon-dispersion relations observed along several symmetric directions in the disordered phase. The solid curves are calculated ones based on a rigid-ion model using the same force constants as in illustrated in Ref. 19: the short-range force constants are taken from Ref. 25 and the Coulombic part is calculated by Ewald's method.

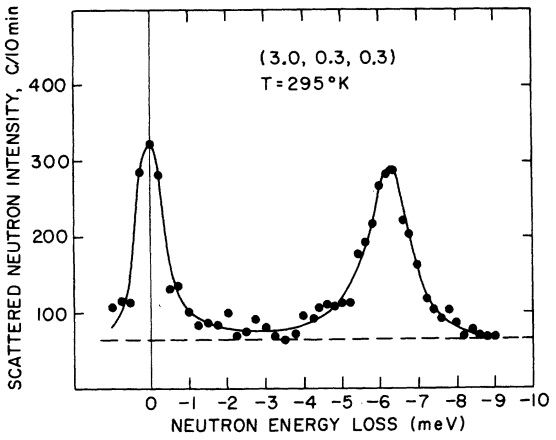

FIG. 3. Typical scattered neutron spectrum observed along the $[0\zeta\zeta]$ direction. In the figure, the elastic incoherent component is subtracted, so that "central peak" represents the response due to fluctuations of orientation of the ND_4^+ ions as well as displacement of the Br^- ions.

$\zeta = 0.20$ in the $[0\zeta\zeta]$ direction. By scanning along the $(-0.04, \zeta, \zeta)$ line (namely, 0.04 off from the exact $[0\zeta\zeta]$ line), we were able to eliminate contamination due to Bragg "tails". The diffuse quasielastic scattering was not affected by this off-set because of the broader nature of its distribution. In Fig. 5, the $\vec{k}$ dependence of the intensities of the quasielastic component thus obtained are plotted along the $[\zeta 00]$, $[0\zeta\zeta]$, and $[\zeta\frac{1}{2}\frac{1}{2}]$ direction. Data given by open circles appearing in the region of $0.1 < \zeta < 0.25$ are obtained from scanning along exact $[0\zeta\zeta]$ line, which is contaminated by Bragg tails. On the other hand, the solid circles in the same region correspond to the data obtained by scanning along $(-0.04, \zeta, \zeta)$ around (300).

The temperature dependence of the spectra were also investigated. Some of the spectra obtained at $(3, \frac{1}{2}, \frac{1}{2})$ are given in Fig. 6. It can be seen that the quasielastic component critically increases at the M point as the temperature is lowered toward the transition temperature, whereas the phonon side peak stays essentially unchanged throughout the temperature region of $T_c + 5\ ^\circ\mathrm{K} < T < T_c + 80\ ^\circ\mathrm{K}$. It has been previously observed by x-ray scattering[11,27] and double-axis-type neutron measurement[12] that the diffuse scattering around M point show the critical behavior. It has now been confirmed that the critical scattering is quasielastic and no critical softening of the phonon branch takes place in the vicinity of the transition temperature.

We have tried to observe the temperature dependence as well as the $\vec{k}$ dependence of the line widths of the quasielastic peak and the phonon peaks. The observed width of the quasielastic component is within the limit of the instrumental resolution throughout the region of $220 < T < 300\ ^\circ\mathrm{K}$ and of $0.15 \leq \zeta < 0.5$ along the $[\zeta\zeta 0]$ direction. On the other hand, the width of phonon peaks shows strong $\vec{k}$ dependence. As is shown in Fig. 4, the width of the TA_2 phonon branch measured along the $[0\zeta\zeta]$ direction increases rapidly as $\zeta \to 0.5$ and reaches

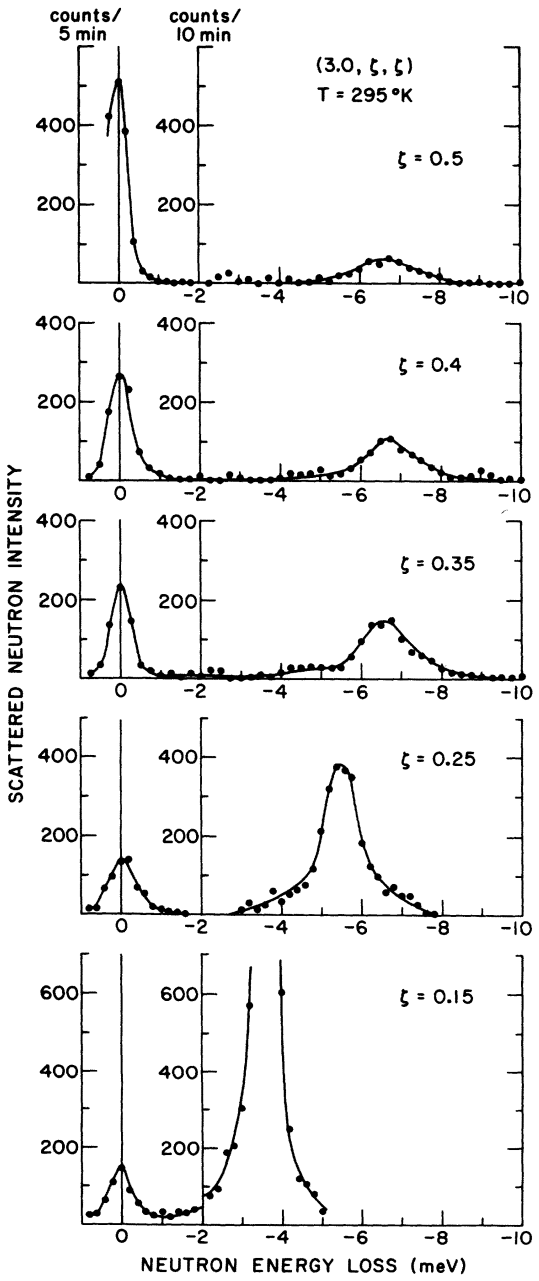

FIG. 4. Wave-number dependence of the scattered neutron spectra observed along the $[0\zeta\zeta]$ line around the (3, 0, 0) reciprocal lattice point. The incoherent background is subtracted.

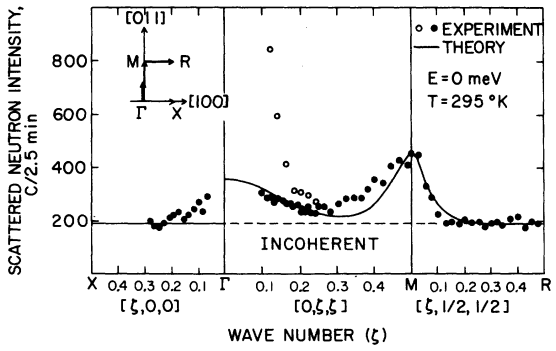

FIG. 5. Quasielastic component observed along several symmetric directions. The open circles plotted in the region of $0.1 < \zeta < 0.25$ are the data obtained scanning directly through the $[0\zeta\zeta]$ line. The solid circles in the same region correspond to the data obtained by scanning through $(-0.04, \zeta, \zeta)$, as is illustrated in the inserted figure. The solid curve is the theoretical one calculated with Eq. (13). The values of $g(\vec{k})$, $J(\vec{k})$ and $\omega(\vec{k})$, given in Ref. 19 are utilized for the calculation. The calculated value is normalized to the observed one at the M point.

maximum value at the M point. As will be discussed later, part of the broadening is considered to be due to the coupling of this mode with the spin system. For comparison, the width of TA_1 phonon at the M point was also observed, the result being included in Fig. 10. The width of the TA_2 branch did not show any appreciable temperature dependence even in the critical region of the phase transition. (See Fig. 6.)

III. CORRELATION FUNCTIONS AND NEUTRON SCATTERING CROSS SECTIONS

The critical dynamical behavior of the pseudospin phonon coupled system was recently studied by Yamada *et al.*[23] Starting from the same Hamiltonian as is given in Eq. (1), they have given explicit expressions for correlation functions, $\phi_{\sigma\sigma}(\vec{K}, \omega)$, $\phi_{\sigma Q}(\vec{k}, \omega)$ and $\phi_{QQ}(\vec{k}, \omega)$, which represent the spin-spin correlation, the spin-phonon correlation, and the phonon-phonon correlation, respectively. Since neutrons are sensitive to both the movement of ND_4^+ groups and Br^- ions, the scattering cross section from ND_4Br is expressed in terms of these three correlation functions.

We proceed to find the expressions for the neutron scattering cross sections based on these expressions for the correlation functions. The neutron-scattering cross section is expressed as the Fourier transformed correlation function of time-dependent structure factors

$$\frac{d^2\sigma}{d\Omega d\omega} = \frac{k'}{k} \int_{-\infty}^{\infty} \langle F(\vec{K}, t) F(-\vec{K}, 0) \rangle e^{-i\omega t} dt \quad , \tag{2}$$

where $\vec{K}$ is the scattering vector, $\vec{k} - \vec{k}$, and k and k' are the absolute values of incident wave vector, $\vec{k}$, and scattered wave vector, $\vec{k}'$, respectively. The time dependence of the structure factor is due to the flipping motion of ND_4^+ groups, as well as the displacement of ND_4^+ ions as a unit and that of Br^- ions. Therefore, the structure factor is given as follows:

$$F(\vec{K}, t) = \sum_i \bar{F}_{ND_4}(\vec{K}) e^{i\vec{K}\cdot\vec{r}_i} + i\Delta F_{ND_4}(\vec{K}) \sum_i \sigma_i(t) e^{i\vec{K}\cdot\vec{r}_i} + i\bar{F}_{ND_4}(\vec{K}) \sum_i \vec{K} \cdot \vec{\Delta}_{i\,ND_4}(t) e^{i\vec{K}\cdot\vec{r}_i} + \sum_i \bar{F}_{Br}(\vec{K}) e^{i\vec{K}\cdot\vec{r}_i}$$
$$+ i\bar{b}_{Br} \sum_i \vec{K} \cdot \vec{\Delta}_{i\,Br}(t) e^{i\vec{K}\cdot\vec{r}_i} \quad . \tag{3}$$

Here, $\vec{\Delta}_{i\,ND_4}(t)$ and $\vec{\Delta}_{i\,Br}(t)$ are the displacement of the ND_4^+ group as a unit and the Br^- ion from their equilibrium position in the ith unit cell. $\bar{F}_{ND_4}(\vec{K})$ and $\Delta F_{ND_4}(\vec{K})$ corresponds to the symmetric and antisymmetric part of the static structure factor of ND_4^+ ion at its equilibrium position, which are given explicitly as follows:

$$\bar{F}_{ND_4}(\vec{K}) = \bar{b}_N + 4\bar{b}_D \cos K_x \frac{\rho}{\sqrt{3}} \cos K_y \frac{\rho}{\sqrt{3}} \cos K_z \frac{\rho}{\sqrt{3}} \quad , \tag{4}$$

$$\Delta F_{ND_4}(\vec{K}) = -4\bar{b}_D \sin K_x \frac{\rho}{\sqrt{3}} \sin K_y \frac{\rho}{\sqrt{3}} \sin K_z \frac{\rho}{\sqrt{3}} \quad . \tag{5}$$

Here $\bar{b}_N$ and $\bar{b}_D$ are the scattering amplitudes of nitrogen and deuterium including the Debye-Waller factors and ρ is the N-D bond length. $\bar{F}_{Br}(\vec{K})$ is the static structure factor of the Br^- ion given by

$$\bar{F}_{Br}(\vec{K}) = \bar{b}_{Br} e^{i\vec{K}\cdot\vec{r}_{0Br}} \quad ,$$

with $\bar{b}_{Br}$ the scattering amplitude of bromine nucleus. It is convenient to introduce Fourier transformed coordinates $\sigma(\vec{k})$ and $Q(\vec{k})$ as follows:

$$\sigma_i(t) = \frac{1}{\sqrt{N}} \sum_{\vec{k}} \sigma(\vec{k}, t) e^{i\vec{k}\cdot\vec{r}_i} \tag{6}$$

$$\vec{\Delta}_{i\,ND_4}(t) = \frac{1}{\sqrt{N}} \sum_{\vec{k}} \frac{\vec{e}_{ND_4}(\vec{k})}{2\sqrt{m_{ND_4}}} \times \{Q(\vec{k}, t) e^{i\vec{k}\cdot\vec{r}_i} + Q^*(\vec{k}, t) e^{i\vec{k}\cdot\vec{r}_i}\} \quad , \tag{7}$$

$$\vec{\Delta}_{i\,\mathrm{Br}}(t)=\frac{1}{\sqrt{N}}\sum_{\vec{k}}\frac{\vec{e}_{\mathrm{Br}}(\vec{k})}{2\sqrt{m_{\mathrm{Br}}}}\times\{Q(\vec{k},t)e^{i\vec{k}\cdot\vec{r}_i}+Q^*(\vec{k},t)e^{-i\vec{k}\cdot\vec{r}_i}\}\quad,\tag{8}$$

where $\vec{e}_{\mathrm{ND_4}}(\vec{k})$ and $\vec{e}_{\mathrm{Br}}(\vec{k})$ are the polarization vectors of the ND_4^+ group and the Br^- ion belonging to the TA_2 branch. The displacement due to the excitation of other phonon branches is neglected, as we are interested in the coupling between this particular mode and the pseudospin coordinate. The neutron-scattering cross section due to fluctuations of atoms is given in terms of the three correlation functions, $\phi_{\sigma\sigma}$, ϕ_{QQ}, and $\phi_{Q\sigma}$ as follows:

$$\frac{d^2\sigma}{d\Omega d\omega}=N\frac{k'}{k}\left[(\Delta F_{\mathrm{ND_4}}(\vec{K}))^2\,\phi_{\sigma\sigma}(\vec{k},\omega)+\left|\bar{F}_{\mathrm{ND_4}}(\vec{K})\frac{\vec{K}\cdot\vec{e}_{\mathrm{ND_4}}(\vec{k})}{\sqrt{m_{\mathrm{ND_4}}}}+\bar{F}_{\mathrm{Br}}(\vec{K})\frac{\vec{K}\cdot\vec{e}_{\mathrm{Br}}(\vec{k})}{\sqrt{m_{\mathrm{Br}}}}\right|^2\phi_{QQ}(\vec{k},\omega)\right.$$
$$+\Delta F_{\mathrm{ND_4}}(\vec{K})\left(\bar{F}_{\mathrm{ND_4}}(\vec{K})\frac{\vec{K}\cdot\vec{e}_{\mathrm{ND_4}}(\vec{k})}{\sqrt{m_{ND_4}}}+\bar{F}_{\mathrm{Br}}(\vec{K})\frac{\vec{K}\cdot\vec{e}_{\mathrm{Br}}(\vec{k})}{\sqrt{m_{\mathrm{Br}}}}\right)\phi_{Q\sigma}(\vec{k},\omega)+\Delta F_{\mathrm{ND_4}}(\vec{K})\left(\bar{F}_{\mathrm{ND_4}}(\vec{K})\frac{\vec{K}\cdot\vec{e}_{\mathrm{ND_4}}(\vec{k})}{\sqrt{m_{\mathrm{ND_4}}}}\right.$$
$$\left.\left.+\bar{F}^*_{\mathrm{Br}}(\vec{K})\frac{\vec{K}\cdot\vec{e}_{\mathrm{Br}}(\vec{k})}{\sqrt{m_{\mathrm{Br}}}}\right)\phi_{\sigma Q}(\vec{k},\omega)\right]\quad,\tag{9}$$

where $\vec{K}=\vec{K}_h+\vec{k}$. Referring to Eqs. (15), (16), and (17) in Ref. 23, the above expression is rewritten in a more convenient form:

$$\frac{d^2\sigma}{d\Omega d\omega}=N\frac{k'}{k}\left|\Delta F_{\mathrm{ND_4}}(\vec{K})+\left(\bar{F}_{\mathrm{ND_4}}(\vec{K})\frac{\vec{K}\cdot\vec{e}_{\mathrm{ND_4}}(\vec{k})}{\sqrt{m_{\mathrm{ND_4}}}}+\bar{F}_{\mathrm{Br}}(\vec{K})\frac{\vec{K}\cdot\vec{e}_{\mathrm{Br}}(\vec{k})}{\sqrt{m_{\mathrm{Br}}}}\right)\frac{\omega_0(\vec{k})g(\vec{k})}{\omega^2-\omega_0^2(\vec{k})}\right|^2\phi_{\sigma\sigma}(\vec{k},\omega)\quad.\tag{10}$$

The expression of $\phi_{\sigma\sigma}(\vec{k},\omega)$ has been given in Ref. (23) as follows:

$$\phi_{\sigma\sigma}(\vec{k},\omega)=\frac{2\gamma k_B T}{\omega^2+\gamma^2(k_BT-J(\vec{k})+\{\omega_0^2(\vec{k})g^2(\vec{k})/[\omega^2-\omega_0(\vec{k})]\})^2}\tag{11}$$

The $\vec{k}$ dependence of $J(\vec{k})$, $g^2(\vec{k})$, and $\omega_0(\vec{k})$ are already given in Ref. 19. Therefore, the above formulas give explicitly the wave-number dependence and the temperature dependence of the neutron scattering cross section, leaving the only parameter γ to be fixed by comparison with experimental results. The parameter γ is related to the relaxation time τ_0 of the flipping of an "independent" spin (that is, the relaxation time of the flipping of individual spin when there are no interactions between other spins as well as phonons) by the relation

$$\gamma=1/k_BT\tau_0\quad.\tag{12}$$

Hereafter, we refer to γ by introducing the dimensionless parameter γ_s defined by

$$\gamma_s\equiv\hbar\gamma\quad.$$

IV. ANALYSIS OF THE EXPERIMENTAL RESULTS

A. Quasielastic scattering

In Eq. (10), we note that the cross section at $\vec{k}=\vec{k}_0\equiv(\frac{1}{2},\frac{1}{2},0)$ and $\omega=0$ is given by

$$\left(\frac{d^2\sigma}{d\Omega d\omega}\right)_{\vec{k}=\vec{k}_0}=\left|\Delta F_{\mathrm{ND_4}}(\vec{K}_0)-\bar{F}_{\mathrm{Br}}(\vec{K}_0)\frac{\vec{K}_0\cdot\vec{e}_{\mathrm{Br}}(\vec{k}_0)}{\sqrt{m_{\mathrm{Br}}}}\frac{g(\vec{k}_0)}{\omega_0(\vec{k}_0)}\right|^2\times\phi_{\sigma\sigma}(\vec{k}_0,0)\quad,\tag{13}$$

where $\vec{K}_0=\vec{K}_h+\vec{k}_0$. Here we have used the fact that

$$\vec{e}_{\mathrm{ND_4}}(\vec{k}_0)=0\tag{14}$$

for this particular phonon branch. On the other hand, the equilibrium displacement of the Br^- ion in the ordered phase (γ phase) is given by[19]

$$\vec{\Delta}_{0\,\mathrm{Br}}=\frac{\vec{e}_{\mathrm{Br}}(\vec{k}_0)}{\sqrt{m_{\mathrm{Br}}}}\frac{g(\vec{k}_0)}{\omega_0(\vec{k}_0)}\quad.\tag{15}$$

Therefore, Eq. (12) is rewritten

$$\left(\frac{d^2\sigma}{d\Omega d\omega}\right)_{\substack{\vec{k}=\vec{k}_0\\ \omega=0}}=|F_\gamma(\vec{K}_0)|^2\,\phi_{\sigma\sigma}(\vec{k}_0 0)\quad;\tag{16}$$

that is, the cross section of the elastic component of the critical scattering at the M point is proportional to the static structure factor of the super-lattice reflection appearing in the γ phase. In Fig. 7, the quasielastic scattering cross sections at various M points observed at 220 °K are compared with the calculated value using Eq. (16) and the equilibrium displacement of the Br^- ion observed at $T=195$ °K.[6] As the temperature factors included in $F_\gamma(\vec{K}_0)$, we have used the values given by Levy and and Peterson: $B_N=1.7$ Å^2, $B_{\mathrm{Br}}=1.7$ Å^2, and $B_D=2.5$ Å^2.[6] The agreement indicates the validity of the model and it implies that the quasielastic com-

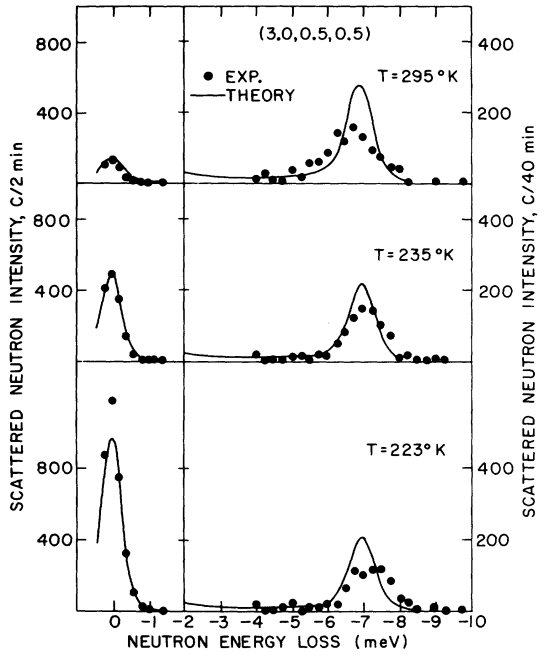

FIG. 6. Temperature dependence of the scattered neutron spectra observed at $(3, \frac{1}{2}, \frac{1}{2})$ (M point). The incoherent background is subtracted. Solid curves are the theoretical ones calculated with Eq. (10) taking $\gamma_s = 0.016$. The calculated value is normalized at $\omega = 0$ of the spectrum obtained at $T = 235\,°K$.

ponent is due to coupled motion of the ND_4^+ ions and the Br^- ions that move in the phase relation explained in Fig. 8.

Furthermore, in Eq. (11) we notice that

$$\phi_{\sigma\sigma}(\vec{k}, 0) = \frac{2k_B T}{\gamma[k_B T - J_{\text{eff}}(\vec{k})]^2} \quad , \tag{17}$$

$$\propto \chi^2(\vec{k}, 0) \quad , \tag{18}$$

$$J_{\text{eff}}(\vec{k}) = J(\vec{k}) + g^2(\vec{k}) \quad . \tag{19}$$

Here $\chi(\vec{k}, 0)$ is the static staggered susceptibility describing the response of pseudospin to the applied fictitious "field" with wave vector $\vec{k}$. In Ref. 19, it is emphasized that it is essential to have two local maxima at the Γ point and the M point in $J_{\text{eff}}(\vec{k})$ in order to explain two successive phase transitions in this substance. It is also pointed out that $J_{\text{eff}}(\vec{k})$ will be strongly anisotropic around the M point and will show a "ridge" along the $[0\zeta\zeta]$ direction. Since the quasielastic component is proportional to $\phi_{\sigma\sigma}(\vec{k}, 0)$, it should reflect these characteristics of $J_{\text{eff}}(\vec{k})$. The observed $\vec{k}$ dependence of the quasielastic component does show the predicted feature. In Fig. 4, we give the observed quasielastic component around the (3, 0, 0) reciprocal lattice point along with the theoretical curve as calculated with Eq. (13). In the calculation, the values of $J(\vec{k})$, $g^2(\vec{k})$, and $\omega_0(\vec{k})$ are taken from Ref. 19. No adjustable parameters are included except that it is normalized at the M point to the observed intensity.

B. Spectra of scattered neutrons: Wave-vector dependence

In the preceding section, it has been demonstrated that the central component of the scattered neutron spectra is due to the correlated mode of the flipping of the ND_4^+ ions and the shift of the Br^- ions. On the other hand, we have also observed a well-defined TA_2 phonon branch at the M point, whose eigenvector exactly corresponds to the spontaneous displacement of the Br^- ion in the static structure in the γ phase. These facts mean that the spectrum of the displacement-displacement correlation of the Br^- ion shows a "triple-peak" structure. Therefore, the dynamical process concerning pseudospins and phonons in ND_4Br must certainly be understood as belonging to the "slow-relaxation" case shown in Fig. 1(a). The criterion of "slow relaxation" is given by $\tau_0^{-1} \ll \omega_0$.

In order to present a more quantitative argument, we use Eqs. (10) and (11) and try to directly compare the observed spectra of the scattered neutrons with the theoretical values. The expression of Eq. (11) contains only one parameter γ which is related to τ_0 by Eq. (12). To determine this parameter, we proceed as follows. In the slow-relaxation case, the parameter γ is expected to be determined by

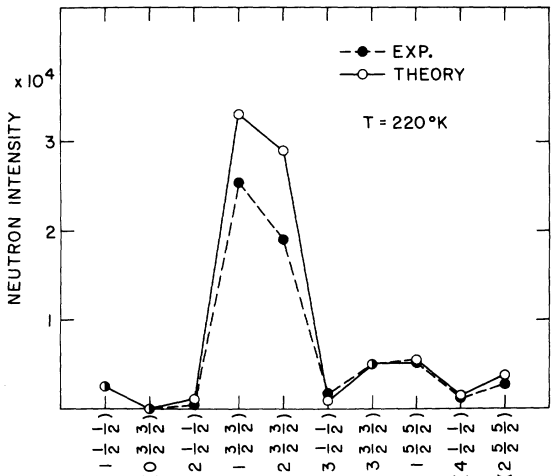

FIG. 7. Comparison of the observed relative and the oretical intensities calculated with Eq. (16) at various M points. The dynamical structure factor is calculated based on the static structure in the low-temperature phase given by Levy and Peterson (Ref. 6). The Debye-Waller factors given by them are utilized. The calculated values is normalized to the observed value at $(3, \frac{3}{2}, \frac{3}{2})$.

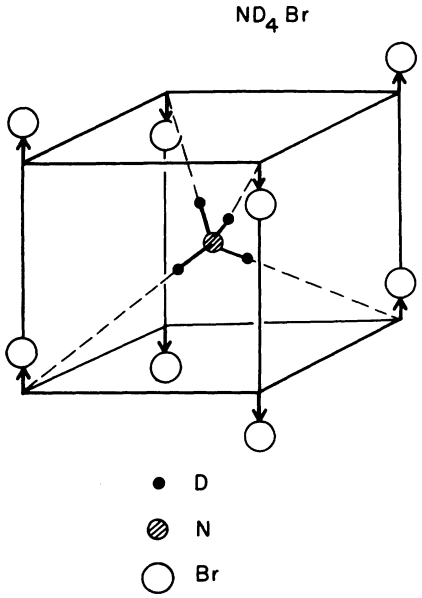

FIG. 8. "Mode" of the coupled relaxational motion of ND_4^+ and Br^-. Neighboring Br^- ions tend to move towards deuterium following the flipping motion of ND_4^+ ions.

the line width of the central peak and that of the side peaks. However, the observed width of the central component was within the limit of instrumental resolution even at 295 °K and did not allow any accurate estimation of the instrinsic width. Moreover, the width of the side peaks includes the broadening due to origins other than the spin-phonon coupling. Under these circumstances, we can only set an upper limit on the value of γ. We estimated the instrumental resolution function following the method developed by Cooper and Nathans.[28] It was then folded to the calculated spectrum around the central peak to compare with the observed line shape. From the condition that the folded line shape agrees with the observed one within the estimated experimental errors, we put the upper limit of the value of γ as $\gamma_s \leq 0.016$ at room temperature. This corresponds to taking the relaxation time as $\tau_0 \geq 1.3\times 10^{-12}$ sec. With this limiting value of γ, the scattered cross sections at arbitrary wave numbers are calculated with Eq. (10). The result of the calculation at $T = 295$ °K is summarized in Fig. 9(b), and the corresponding observed spectra are depicted in Fig. 9(a). Although we can not yet directly compare these curves because of the instrumental resolution involved in the observed values, the general agreement between observed and calculated spectra are obvious. Furthermore, we plot the $\vec{k}$ dependence of the linewidth (FWHM) of the side peak obtained from the calculated spectra and compare with the observed linewidths. On carrying out this comparison, the observed linewidths are corrected for the instrumental resolution by assuming that the dispersion surface is planar in the region where neutron probe has finite contribution. The corrected values are also included in Fig. 10. No definite conclusion can be derived from the comparison of the curve with the experimental points, since the latter includes extra broadening due to phonon-phonon interaction etc. In order to estimate the broadening due to other origins, the line width of the TA_1 branch, which does not couple with the spin by the crystal symmetry was also studied. After correction for the instrumental resolution,

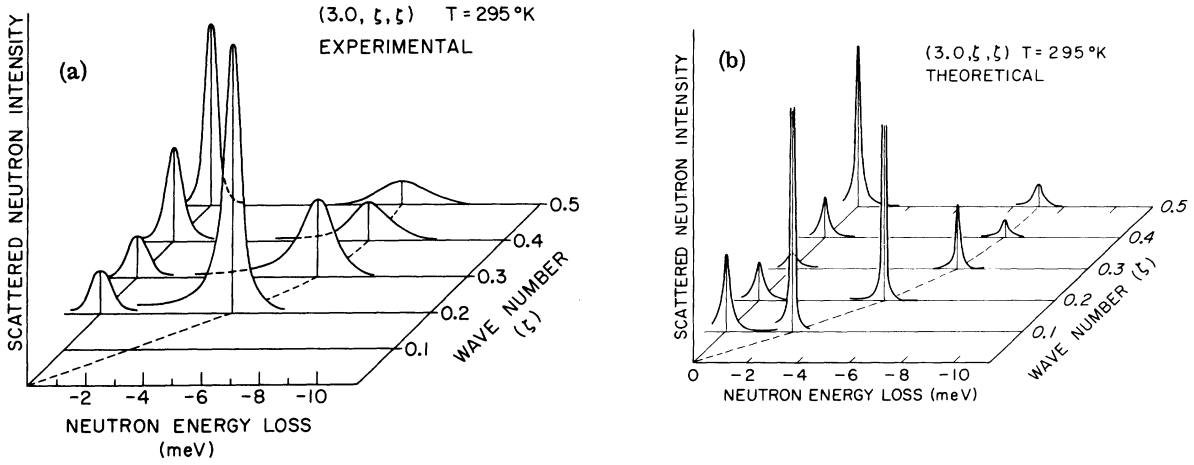

FIG. 9. Wave-number dependence of the neutron spectra along the $[0\zeta\zeta]$ line. Case (a) represents the experimental curves after smoothing out the data points. Case (b) is the corresponding calculated curves for $\gamma_s = 0.016$. The calculated curves are not folded to the resolution functions.

the width is estimated to be 0.7 meV at the zone boundary. Using this value for the intrinsic background width (i.e., due to other than spin-phonon coupling) of the TA_2 branch, the calculated spin-phonon contribution to the linewidth is correct to within a factor of 2 and displays the correct qualitative behavior.

C. Spectra of scattered neutrons: Temperature dependence

In Fig. 6, it is clearly shown that no softening nor broadening of the TA_2-phonon side peak takes place when the temperature is lowered towards the critical temperature. It even shows a small amount of stiffening as normally observed in ordinary ionic crystals. On the other hand, the intensity of the central component increases critically in the vicinity of the transition temperature. The critical scattering previously observed by x-ray scattering[11,27] and double axis neutron scattering[12] is largely this quasielastic component. On observing Fig. 1, one can see the above stated characteristics of the temperature dependence of the spectra are also consistent with the case of "slow relaxation."

We have calculated the temperature dependence of the neutron scattering cross sections at $(3\frac{1}{2}\frac{1}{2})$ with Eq. (10), where the value of γ is taken as $\gamma_s = 0.016$. The calculated curves are then folded with the resolution function for the direct comparison with the observed spectra. The results are shown in Fig. 6 by the solid curves together with the observed points. The calculated curves are normalized to the observed value at the single point $\omega = 0$ and $T = 235\,^{\circ}K$. It is seen that the calculated phonon peaks are considerably narrower than the observed peaks, for the reason which has been discussed in the preceding section. Except for this point, the agreement between the calculated spectra and the observed ones are satisfactory. Especially the principal characteristics—namely, no softening nor broadening of phonon peaks takes place, and the critical enchancement of fluctuations occurs in the central component—are reproduced in the calculated patterns.

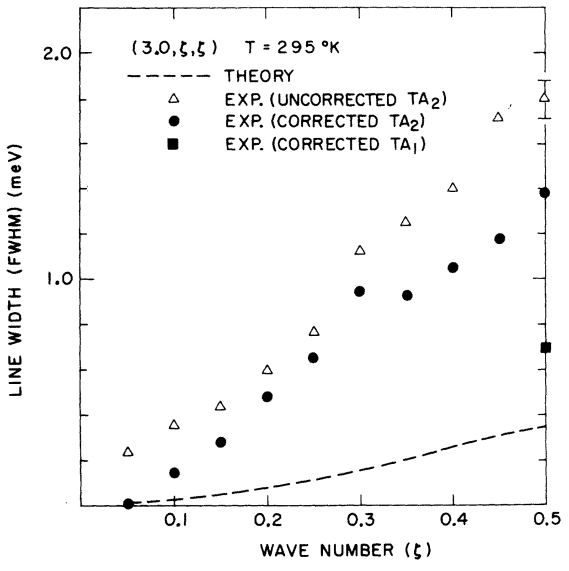

FIG. 10. Linewidth of the neutron spectra due to phonon excitations observed along the $[0\zeta\zeta]$ line. The TA_2 branch includes the effect of broadening due to spin-phonon coupling, whereas the TA_1 branch does not couple with the spin system. The dotted line is the estimated width due to spin-phonon coupling in the TA_2 branch. Solid triangles are the direct observations, and solid circles are the data obtained after the corrections for instrumental resolution.

V. CONCLUSIONS AND DISCUSSIONS

From the dynamical structure factors observed at various M points, we clearly see that part of the displacement of the Br^- ion follows the reorientational motion of the ND_4^+ ion. This motion is characterized as the relaxational motion with relaxation time much longer than the characteristic period of vibration of phonon mode. In addition to the relaxation mode, there exists a well-defined TA_2 phonon mode at the [110] zone boundary whose polarization vector exactly corresponds to the static structure in the lower-temperature phase. However, the softening of the "condensing" phonon mode does not take place in this substance. Instead, the critical enhancement of the fluctuations of the displacement of the Br^- ions is mainly associated with the relaxational part. From these features we conclude that the ND_4Br system falls into the category of the "slow-relaxation" case discussed in Ref. 23.

The theory predicts that the dynamical coupling between spins and phonons will give rise to broadening of the spectra. In the case of ND_4Br, however, we could only set a limiting value to the flipping frequency due to experimental limitations. The result gives that the relaxation time of an "independent" spin τ_0 is longer than 1.3×10^{-12} sec. The effective relaxation time of a spin fluctuation should show a critical slowing-down effect due to interactions between spins and phonons. In Ref. 23, it has been shown that the relaxation time of the spin fluctuation with wave vector $\vec{k}_0$ is given by

$$\tau_{(\vec{k}_0)} = \tau_0[T/(T - T_c)] \quad .$$

Even at room temperature, $\tau_{(\vec{k}_0)}$ is estimated as longer than 0.48×10^{-11} sec, which means that the flipping frequency of spins is about 0.020 of the characteristic frequency of the TA_2 branch at the [110] zone boundary.

Therefore, for the high-frequency phonons, the relaxational fluctuations can be simply considered as static disturbance, by which the equilibrium positions of the Br^- ions are displaced from the high-symmetry site. Recently, Sokoloff and Loveluck[29] treated the phonon system in ammonium halides in particular reference to Raman scattering and neutron scattering effects based on the assumption of static random orientations of ammonium ions. As far as the behavior of the optical phonons and the zone-boundary phonons are concerned, his model seems to be completely valid in the temperature region less than room temperature.

On the other hand, for the low-frequency phenomena such as NMR spectra, the pseudospin fluctuations will give rise to a motional narrowing effect. The observed proton and bromine NMR spectra[14–16] of ammonium halides in the β phase show narrowing due to flipping of ammonium ions. From the observed spin-lattice relaxation time, Gutowsky *et al.*[14] deduced the relaxation time of the flipping at room temperature as $\tau = 5.4 \times 10^{-11}$ sec, which is consistent with our limiting value of $\tau_{(\vec{k}0)} = 0.48 \times 10^{-11}$ sec, although we can not directly compare these values because the neutron observes the relaxation process with a particular $\vec{k}$ value.

It has been shown that the intensity of the quasielastic part of the scattering cross section observed along $[3\zeta\zeta]$ give two maxima: one at the Γ point and the other at the M point. The relative intensity at the M point is higher than at the Γ point. These features are consistent with the scheme of the successive phase transitions in ND_4Br as is discussed in Ref. 19. On the other hand, in ND_4Cl it is known that the parallel ordering of pseudospins develops below the critical point. Since the general property of the interactions between spins and phonons will be similar in both substances, we expect that in ND_4Cl the diffuse scattering along $[0\zeta\zeta]$ will show a similar pattern, except that the relative intensity of the Γ point and the M point is reversed in this case, i.e., the intensity at the Γ point will be higher than that at the M point. It would be interesting to carry out neutron-scattering experiment in ND_4Cl to check this point.

ACKNOWLEDGMENTS

This work is supported in part by the U.S.-Japan Cooperative Science Program performed by the U.S. National Science Foundation and Japan Society for the Promotion of Science. The authors are indebted to M. Blume, D. L. Huber, and S. M. Shapiro for many stimulating discussions. They are also indebted to Professor Kawamori of Kwansei Gakuin University for her help in determination of the deuteration ratio by the use of the NMR technique.

---

†Work supported in part by U. S.-Japan Cooperative Science Program.
*Guest scientist, Brookhaven National Laboratory, 1973.
‡Work performed under the auspices of the U. S. Atomic Energy Commission.

[1]M. Kataoka and J. Kanamori, J. Phys. Soc. Jap. 32, 113 (1972).
[2]R. J. Elliott, R. T. Harley, W. Hayes, and S. P. R. Smith, Proc. Soc. A 328, 217 (1972).
[3]E. Pytte, Phys. Rev. B 3, 3503 (1971).
[4]K. K. Kobayashi, J. Phys. Soc. Jap. 24, 497 (1968).
[5]B. D. Silverman, Phys. Rev. Lett. 20, 443 (1968).
[6]H. A. Levy and S. W. Peterson, J. Amer. Chem. Soc. 75, 1536 (1953).
[7]T. Nagamiya, Proc. Phys. Math. Jap. 24, 137 (1943).
[8]T. Nagamiya, Proc. Phys. Math. Jap. 25, 540 (1943).
[9]A. Bonilla, C. W. Garland, and N. E. Schumaker, Acta Crystallogr. A 26, 156 (1970).
[10]G. Egert, I. R. Jahn, and D. Renz, Solid State Commun. 9, 775 (1971).
[11]H. Terauchi, Y. Noda, and Y. Yamada, J. Phys. Soc. Jap. 32, 1560 (1972).
[12]R. S. Seymour, Acta Crystallogr. A 27, 348 (1971).
[13]C. W. Garland and C. F. Yarnell, J. Chem. Phys. 44, 1112 (1966).
[14]H. S. Gutowsky, G. E. Pake, and R. Bersohn, J. Chem. Phys. 22, 643 (1954).
[15]J. Itoh, R. Kusaka, and Y. Saito, J. Phys. Soc. Jap. 17, 463 (1962).
[16]J. Itoh and Y. Yamagata, J. Phys. Soc. Jap. 17, 481 (1962).
[17]C. H. Wang, Phys. Rev. Lett. 17, 1226 (1971).
[18]J. Weigle and H. Saini, Helv. Phys. Acta 9, 515 (1936).
[19]Y. Yamada, M. Mori, and Y. Noda, J. Phys. Soc. Jap. 32, 1565 (1972).
[20]B. D. Silverman, Phys. Rev. Lett. 25, 107 (1970).
[21]E. Pytte (private communication).
[22]E. Pytte and J. Feder (private communications).
[23]Y. Yamada, H. Takatera, and D. L. Huber, J. Phys. Soc. Jap. (to be published).
[24]H. Mori, Prog. Theor. Phys. 33, 424 (1965).
[25]J. Govindarajan and T. M. Haridasan, Indian J. Pure Appl. Phys. 8, 376 (1970).
[26]H. C. Teh and B. N. Brockhouse, Phys. Rev. B 3, 2733 (1971).
[27]D. Renz, K. Breutner, and H. Dachs, Solid State Commun. 11. 879 (1972).
[28]M. J. Cooper and R. Nathans, Acta Crystallogr. 23, 357 (1967).
[29]J. B. Sokoloff and J. M. Loveluck, Phys. Rev. B 7, 1644 (1973).